ChemComm

Accepted Manuscript

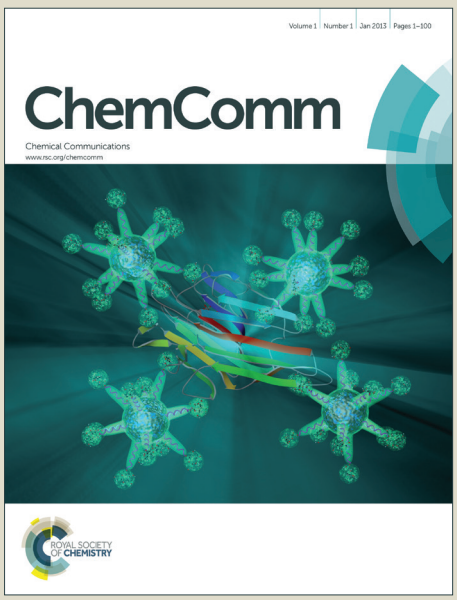

ROYAL SOCIETY OF CHEMISTRY

www.rsc.org/chemcomm

Journal Name

RSCPublishing

COMMUNICATION

A click chemistry approach to site-specific immobilization of a small laccase enables efficient direct electron transfer in a biocathode

Cite this: DOI: 10.1039/xoxxoooooox

Received ooth January 2012,
Accepted ooth January 2012

DOI: 10.1039/xoxxoooooox

www.rsc.org/

Dongli Guan[a], Yadagiri Kurra[c], Wenshe Liu[b*], and Zhilei Chen[a,b*]

Controlled orientation of a small laccase on a multi-walled carbon nanotube electrode was achieved via copper-free click chemistry mediated immobilization. Modification of the enzyme was limited to only the tethering site and involved the genetic incorporation of the unnatural amino acid 4-azido-L-phenylalanine (AzF). This approach enabled efficient direct electron transfer.

Enzyme-based biofuel cells and biosensors promise to be a next-generation energy source for several reasons, including environmental friendliness and renewability[1-3]. However, compared to conventional catalysts employing relatively simple inorganic chemistry, biocatalysts (i.e. enzymes) typically suffer from poor electron transfer and current instability, giving rise to low power densities and short current lifetimes[1, 4]. Proteins are non-conductive and protein matrices can electrically insulate the enzymatic redox center, preventing efficient electron transfer between the enzyme and electrode[4, 5]. Electron transport between the enzyme's catalytic center and the electrode occurs through either direct electron transfer (DET) or mediated electron transfer (MET). In DET, enzymes exchange electrons with the electrode either directly or through a conductive wire, such as a carbon nanotube. Mediated electron transfer relies on a separate, redox-active mediator to shuttle electrons between the enzyme's catalytic center and the electrode. Redox mediators typically suffer from high cost, high toxicity and low stability[6]. Direct electron transfer, on the other hand, is conceptually simple and non-toxic, but efficient direct electrical wiring of enzymes on an electrode or conductive wire is rarely achieved. As a result, the electron harvesting efficiency of DET is usually much lower than that achievable by MET[6, 7].

The electron harvesting efficiency of DET electrodes depends primarily on the distance between the enzyme's catalytic center and the electrode surface[6, 8]. Numerous approaches have been employed to enhance DET between the enzyme and the electrode[9-12]. One commonly pursued strategy is to surround the enzymes in a highly conductive matrix (e.g. a high-surface-area nanomaterial)[11, 13-15]. For example, Zebda et al. physically mixed redox enzymes with multi-walled carbon nanotubes (MWCNTs) and compressed the composite material under high pressure to form an enzyme-MWCNT disk electrode[11]. The heterobifunctional cross-linker, 1-pyrenebutanoic acid succinimidyl ester (PBSE), which forms an amide bond with lysine residues on the protein and interacts with MWCNTs via π–π stacking of the polyaromatic pyrenyl moiety, has been synthesized for immobilizing redox enzymes on carbon electrodes[14, 16]. Another strategy that has been employed to enhance DET is to fabricate modified electrodes that facilitate the strategic orientation of enzyme catalytic sites towards the conductive matrix or electrode surface. For example, aromatic molecules resembling the natural substrate of laccase and bilirubin oxidase have been conjugated to electrode surfaces to enhance the electrocatalytic reduction of oxygen by these enzymes[17, 18]. Unfortunately, this strategy cannot be extended to redox enzymes that do not have easily synthesizable natural substrate mimics. In another example, Banta and coworkers introduced cysteines into different positions in the vicinity of the active site of a glucose oxidase (GOx) and site-specifically attached the enzyme variants to a maleimide-

functionalized gold nanoparticle[19]. A limitation of this approach is the requirement that all the non-targeted free surface cysteines in the enzyme be substituted with non-cysteine residues to ensure single point attachment. Extensive modification of the enzyme in this fashion can negatively impact protein activity.

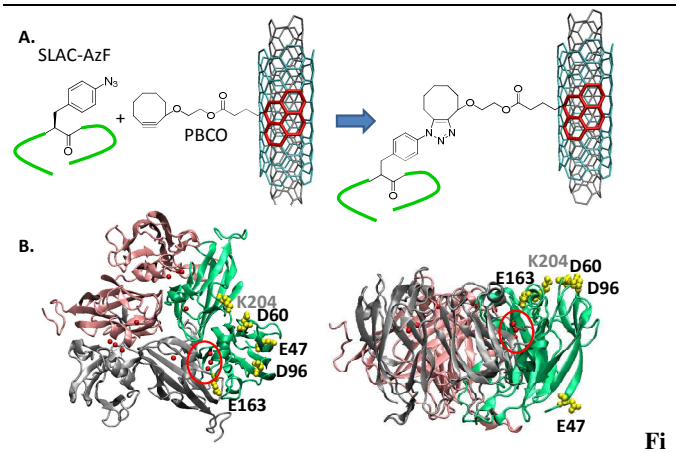

Figure 1. (**A**) Schematic of SLAC immobilization reaction. The heterobifunctional linker PBCO associates with MWCNTs via π–π stacking, and a copper-free click chemical reaction between AzF and a cyclooctyne group on the PBCO linker enables directional immobilization of SLAC (represented by green line) on MWCNTs. (**B**) Top (left diagram) and side (right diagram) views of SLAC trimer. *Red spheres*: catalytic copper ions. *Yellow residues*: candidate sites for AzF incorporation. Residues from only one monomer are depicted (pdb code: 3CG8[20]).

In this study, we sought to develop a facile strategy for the site-specific directional immobilization of enzymes on DET electrodes. An unnatural amino acid 4-azido-L-phenylalanine (AzF) was incorporated into specific sites of a small laccase from Streptomyces coelicolor (SLAC)[21-23]. We chose SLAC because it is easily purified and is known to support DET electrodes[21-23]. A heterobifunctional crosslinker, cyclooctynyloxyethyl 1-pyrenebutyrate (PBCO), was synthesized and used to functionalize MWCNTs on buckypaper via π–π stacking. A copper-free cycloocytyne-azide cycloaddition reaction[24-26] between AzF on the enzyme and cyclooctyne on the MWCNT enabled directional immobilization of SLAC on the buckypaper.

Guided by the crystal structure of SLAC (Figure 1)[20], we identified five candidate sites for the incorporation of AzF. These sites were either in the immediate vicinity of the active site or offered the potential to position the active site within 20 Å of the electrode. To facilitate modification via click chemistry and ensure minimal impact on protein folding/activity, all of these sites were chosen to be at the protein surface. Three of the selected sites (i.e. D60, D96, E163) are located in domain 2 adjacent to the trinuclear copper cluster; and one site E47, is on the opposite site of the protein; and one site K204, is in domain 1 adjacent to copper ion 1. All SLAC variants were expressed as fusions to the Src homology 3 domain (SH3) protein[27] which was previously found to bind carbon nanotubes[28]. SH3-SLAC$_{AzF}$ variants were purified via one-step IMAC except for the K204AzF mutant (Figure S1). The K204AzF mutant was not pursued for further studies because the purified product contained a significant amount of a truncated variant that derives from the use of an amber stop codon for the unnatural amino acid incorporation, and truncated monomers associate with full-length monomers[20]. The yields of the SH3-SLAC$_{AzF}$ mutants were ~30-50% that of the wild-type (WT) enzyme. Accessibility of AzF to the click chemistry reaction was confirmed by incorporation of fluorescently labeled cyclooctyne (Figure S2).

We determined the kinetics of the SH3-SLAC$_{AzF}$ mutants and WT in free solution using 2,6-dimethoxyphenol (DMP) as the substrate[22]. SLAC catalyzes the conversion of DMP into dimeric 3,3',5,5'-tetramethoxydiphenylquinone which absorbs at 468 nm. The measured K_M and K_{cat} for SH3-SLAC$_{WT}$ were 8.74 mM and 0.98 s^{-1} (Figure 3), respectively, representing a comparable catalytic efficiency to that reported for free SLAC (K_M ~3.9 mM and K_{cat} ~0.5 s^{-1})[22]. All SH3-SLAC$_{AzF}$ variants were comparable to SH3-SLAC$_{WT}$ in catalytic activity (K_{cat}) and only D96AzF diverged in catalytic activity by >2-fold (Figure S3).

Table 1. V_{max} and DET efficiency for electrode-immobilized SH3-SLAC AzF mutants and WT.

SH3-SLAC construct		Immobilized enzyme (nmol)[a]	Actively immobilized enzyme (10^{-2} nmol)	V_{max} for DET (10^{-3} nmol/sec)[c]	V_{max} for DMP (10^{-2} nmol/sec)	Electron transfer efficiency (%)[d]
E47AzF	+ PBCO	0.80 ± 0.04[b]	3.65 ± 0.92	5.75 ± 1.34	2.01 ± 0.50	28.7 ± 0.53
	+ PBSE	0.94 ± 0.19	4.30 ± 0.00	0.79 ± 0.38	2.36 ± 0	3.35 ± 1.63
D60AzF	+ PBCO	0.49 ± 0.00	3.36 ± 0.18	2.15 ± 0.18	2.89 ± 0.16	7.45 ± 0.23
	+ PBSE	0.62 ± 0.06	3.58 ± 0.00	0.56 ± 0.13	3.08 ± 0	1.82 ± 0.42
D96AzF	+ PBCO	0.91 ± 0.02	6.15 ± 0.09	0.69 ± 0.02	1.67 ± 0.03	4.12 ± 0.04
	+ PBSE	0.94 ± 0.02	6.01 ± 0.29	0.44 ± 0.11	1.64 ± 0.08	2.69 ± 0.54
E163AzF	+ PBCO	0.96 ± 0.33	5.39 ± 0.23	1.44 ± 0.45	7.59 ± 0.32	1.89 ± 0.52
	+ PBSE	0.87 ± 0.09	5.20 ± 0.11	1.04 ± 0.19	7.32 ± 0.16	1.42 ± 0.22
WT	+ PBCO	0.67 ± 0.16	3.10 ± 0.11	0.40 ± 0.13	4.32 ± 0.16	0.94 ± 0.33
	+ PBSE	0.50 ± 0.09	3.16 ± 0.19	0.60 ± 0.07	4.39 ± 0.27	1.36 ± 0.08

[a] Errors represent the standard deviation of readings derived from duplicate electrodes.

[b] Electron transfer efficiency is calculated by dividing V_{max} for DET with V_{max} for DMP.

For electrode immobilization, compressed MWCNT buckypaper (5 mm x 5 mm) was first glued onto an indium-tin oxide (ITO) electrode using silver conductive epoxy glue for mechanical reinforcement, and the MWCNT-functionalized electrode was gently rocked in a solution containing PBCO or PBSE (10 mM in DMSO) at room temperature for 1 hr to allow the polyaromatic pyrenyl moiety on the heterobifunctional linker to associate with the MWCNT through π-π stacking. Linker-functionalized buckypaper electrode was then incubated with individual enzymes (2 mg/mL in 200 mM NaCl, 50 mM NaPOi, pH 7.4) overnight to enable the cyclooctyne-AzF click reaction (PBCO linker) or amine-succinimide reaction (PBSE linker) to proceed. It is noteworthy that some enzyme will likely associate with the carbon nanotubes non-specifically, regardless of these targeted immobilization reactions[29]. The concentration of enzyme in the solution following the immobilization reaction was measured 12-14 hours later and used to estimate the amount of enzyme immobilized on the electrode. A comparable amount of total enzyme (0.49-0.96

nmol) and active enzyme was immobilized on the electrodes, regardless of the chemistry of the linker and the mutation (Table 1).

Following the completion of the enzyme activity assay, electrodes were immediately subjected to a chronoamperometric (CA) assay for determination of the supported DET current[11]. Enzyme-modified PBCO- and PBSE-electrodes were immersed in 20 mL Buffer C with N_2 or O_2 sparging through the solution. The CA current was recorded at 0.2 V vs. standard hydrogen electrode (SHE). The catalytic current was calculated by subtracting the background N_2 saturation current from the plateau O_2 saturation current and used to determine V_{max} for DET. The electron transfer efficiency was calculated by dividing the V_{max} value calculated from the DET current by that obtained using DMP as the substrate[15]. For the PBSE-modified electrodes, only <3.4% of the actively immobilized enzyme was electrically wired onto the modified electrode, regardless of the site of AzF incorporation. This low electron transfer efficiency is consistent with that reported for other PBSE-modified electrodes[15]. In contrast, a much higher electron transfer efficiency of 28.7% was obtained for E47AzF SH3-SLAC on the PBCO-modified electrode (Table 1, S2, Figure 2). No O_2 responsive current was obtained with PBSE/PBCO-modified electrode in the absence of laccase (Figure S4). It is noteworthy that SLAC is a trimeric protein with diameter < 8 nm[20] and the average distance between different MWCNT in buckypaper is ~100 nm. Thus, it is likely that only one of the monomers of the trimeric protein can be correctly oriented onto the electrode via the PBCO linker. Under this single monomer tethering assumption, the effective maximum electron transfer efficiency for SH3-SLAC is only 33.3%. Thus, the 28.7% transfer efficiency achieved by E47AzF SH3-SLAC on the PBCO-modified electrode suggests that a large percentage of the actively immobilized E47AzF SH3-SLAC may accept electrons from the electrode unhindered. The second highest electron transfer efficiency in our study, 7.5%, was obtained for D60AzF SH3-SLAC on the PBCO-modified electrode. In this case, too, the PBCO linker enabled superior (~4-fold enhanced) electron transfer relative to PBSE. The choice of PBCO vs. PBSE linker did not significantly impact the electron transfer capability of the other two mutants or WT SH3-SLAC.

The high electrical wiring efficiency for E47AzF is somewhat unexpected. Each SLAC monomer contains four copper ions: one type I copper ion in domain 1 and one trinuclear copper cluster in domain 2. The presence of substrates initiates a catalytic cycle near the type I copper ion, generating four electrons (produced by oxidation of four substrate molecules) that are then sequentially transferred to the trinuclear copper cluster and used to reduce an oxygen molecule to water to complete the cycle[20]. In DET electrodes, the electrons are provided by the electrode directly to the trinuclear copper cluster for oxygen reduction. Based on this information, we hypothesized that orienting the enzyme's trinuclear copper cluster closer to the electrode would facilitate more efficient electron transfer. Most of the AzF sites were thus selected to be adjacent to the trinuclear copper cluster on the apical side of the protein (Figure 1B), except for residue E47, which is on the basal side of the protein and was originally intended as the negative control. The distances between the AzF-modified residues and the type I copper and the trinuclear copper cluster are shown in Table S3, with E163AzF and E47AzF being the closest and farthest residues to the copper sites, respectively. Surprisingly, E163AzF exhibited the lowest electron transfer efficiency while E47AzF yielded the highest efficiency. Further study of the SLAC crystal structure revealed a water channel connecting the trinuclear copper cluster and the basal surface of the protein (Figure S5). Anchoring enzyme via E47 potentially brings the carbon nanotube adjacent to this water channel. Previously, molecular dynamics studies showed that structured water molecules can substantially enhance electron transfer rate between the donor and the acceptor[30]. Thus, proximity to this water channel may account for the high electron transfer efficiency of E47AzF. This result underscores the value of AzF-mediated site-specific immobilization as a tool to evaluate the DET efficiency of enzymatic electrodes, since the approach provides the flexibility to attach enzymes to electrodes using potentially any protein residue as an anchor site.

To determine the stability of the enzyme-modified electrode, E47AzF-modified PBCO- and PBSE-electrodes were stored in Buffer C at room temperature for 1 week and CA measurement of the DET current was repeated. The catalytic current generated by the E47AzF-SH3-SLAC-modified PBCO-electrode was 8.85 ± 2.05 and 7.68 ± 1.96 $\mu A/cm^2$ on day 0 and day 8, respectively, indicating a 13.6% reduction in current density over 8 days (Figure 2, Table S2). In contrast, the catalytic current generated by E47AzF SH3-SLAC on the PBSE-modified electrode deteriorated by 47.0% within the same period. Taken together, these data suggest that the PBCO-AzF-mediated click chemistry conjugation of enzymes to electrodes may not only improve electron transfer on DET electrodes, but also extend the enzyme half-life relative to the non-specific amine-succinimide crosslinking mediated by PBSE.

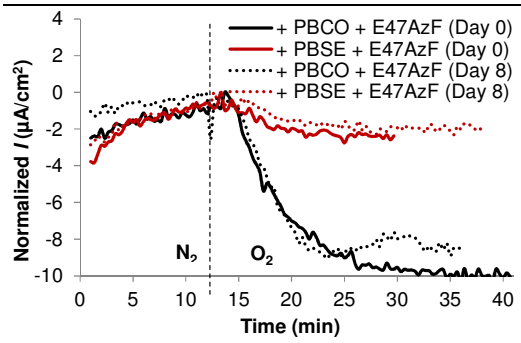

Figure 2. Chronoamperometric measurement of DET current at 0.2 V vs. SHE. PBSE- and PBCO-modified electrodes were functionalized with 2 mg/ml E47AzF SH3-SLAC. The background current density after N_2 saturation was normalized to 0.

Finally, we examined the effect of enzyme concentration on the performance of the PBCO-functionalized buckypaper electrodes. Electrodes modified with 10 and 20 mg/mL of

E47AzF SH3-SLAC contained 1.46 and 2.27 nmol of immobilized enzyme, and the amount of actively immobilized enzymes were $8.41x10^{-2}$ and $11.5x10^{-2}$ nmol, respectively (Figure S4). In comparison, PBCO-modified electrode exposed to only 2 mg/mL E47AzF SH3-SLAC contained 0.80 nmol of total immobilized enzyme and 3.65 $x10^{-2}$ nmol actively immobilized enzyme (Table 1). The catalytic current from CA measurement on electrodes modified with 10 and 20 mg/mL E47AzF SH3-SLAC were 20.88 ± 0.42 and 18.61 ± 1.33 $\mu A/cm^2$, respectively, significantly higher than that generated from electrode modified with 2 mg/mL E47AzF (8.85 ± 2.05 $\mu A/cm^2$, Figure S4). However, despite the higher catalytic currents obtained with electrodes modified with the higher concentrations of enzyme, a drop in electrical wiring efficiency from 28.7% to 13.3% was observed when the E47AzF SH3-SLAC concentration was increased from 2mg/mL to 20 mg/mL. This finding is not surprising as only a limited conductive surface area is available on MWCNTs and excessive protein may insulate the enzyme's catalytic site.

Conclusions

In summary, this study presents a facile click chemistry-based strategy to site-specifically immobilize redox enzymes on DET electrodes in a way that supports both enhanced electron transfer and a stable current. This study employed SLAC as the redox enzyme because SLAC can be easily expressed and purified from *E. coli*, a desirable trait for high efficiency incorporation of unnatural amino acid. The unnatural amino acid AzF can be readily incorporated into virtually any site within a protein and its reaction with cyclooctyne is highly specific[31]. This approach requires modification of the enzyme at only the tethering site, in contrast to methods of site-specific immobilization that rely on the surface presence of amino acids with a given chemistry (eg. thiols on cysteines[19]). In the latter approach non-targeted residues must be substituted to enable site-specific attachment, at the risk of negatively impacting protein performance. In the present study, incorporation of AzF had only a relatively minor impact on enzyme kinetics (≤2-fold). The copper-free click chemistry reaction exploited to attach the enzyme to the PBCO-modified electrodes is highly efficient and allows for flexibility in design. In particular, the click chemistry approach allows the distance between the enzyme and the electrode to be altered simply by adjusting the length of the linker. A remarkably high DET efficiency and a stable current that deteriorated only ~14% following 8 days of solution-phase incubation at ambient temperature was achieved with the electrode containing the click-incorporated E47AzF variant of SLAC. The approach of using click chemistry for electrode immobilization can be easily applied to other redox enzymes and a much higher catalytic current can potentially be obtained when more efficient redox enzymes are employed. We envision that the described approach could provide a powerful, enabling tool for creating the next generation high-efficiency DET electrodes for use in biofuel cells and biosensors.

Notes and references

[a] Chemical Engineering Department, Texas A&M University,
[b] Department of Microbial Pathogenesis & Immunology, Texas A&M University Health Science Center, College Station, TX 77843. E-mail: zchen4@tamu.edu; Tel: +1 979-436-9404
[c] Department of Chemistry, Texas A&M University, College Station, TX 77843. wliu@chem.tamu.edu; Tel: +1 979-845-1746

† Electronic supplementary information (ESI) available: Experimental details and supplementary figures. See DOI: 10.1039/c000000x/

1. R. A. Bullen, T. C. Arnot, J. B. Lakeman and F. C. Walsh, *Biosens Bioelectron*, 2006, **21**, 2015-2045.
2. S. A. Neto, J. C. Forti and A. R. De Andrade, *Electrocatalysis*, 2010, **1**, 87-94.
3. A. Sassolas, L. J. Blum and B. D. Leca-Bouvier, *Biotechnol. Adv.*, 2012, **30**, 489-511.
4. J. Kim, H. Jia and P. Wang, *Biotechnol Adv*, 2006, **24**, 296-308.
5. E. H. Yu and K. Scott, *Energies*, 2010, **3**, 23-42.
6. M. T. Meredith and S. D. Minteer, *Annual review of analytical chemistry*, 2012, **5**, 157-179.
7. M. C. Beilke, T. L. Klotzbach, B. L. Treu, D. Sokic-Lazic, J. Wildrick, E. R. Amend, L. M. Gebhart, R. L. Arechederra, M. N. Germain, M. J. Moehlenbrock, Sudhanshu and S. D. Minteer, in *Micro Fuel Cells: Principles and Applications*, 2009, pp. 179-241.
8. A. L. Ghindilis, P. Atanasov and E. Wilkins, *Electroanal*, 1997, **9**, 661-674.
9. P. Wu, Q. A. Shao, Y. J. Hu, J. A. Jin, Y. J. Yin, H. Zhang and C. X. Cai, *Electrochim Acta*, 2010, **55**, 8606-8614.
10. J. Zhang, M. Feng and H. Tachikawa, *Biosens Bioelectron*, 2007, **22**, 3036-3041.
11. A. Zebda, C. Gondran, A. Le Goff, M. Holzinger, P. Cinquin and S. Cosnier, *Nat Commun*, 2011, **2**, 370.
12. S. Rubenwolf, O. Strohmeier, A. Kloke, S. Kerzenmacher, R. Zengerle and F. von Stetten, *Biosens Bioelectron*, 2010, **26**, 841-845.
13. T. Miyake, S. Yoshino, T. Yamada, K. Hata and M. Nishizawa, *J Am Chem Soc*, 2011, **133**, 5129-5134.
14. A. Szczupak, J. Halamek, L. Halamkova, V. Bocharova, L. Alfonta and E. Katz, *Energ Environ Sci*, 2012, **5**, 8891-8895.
15. L. Halamkova, J. Halamek, V. Bocharova, A. Szczupak, L. Alfonta and E. Katz, *J Am Chem Soc*, 2012, **134**, 5040-5043.
16. R. P. Ramasamy, H. R. Luckarift, D. M. Ivnitski, P. B. Atanassov and G. R. Johnson, *Chem Commun (Camb)*, 2010, **46**, 6045-6047.
17. M. T. Meredith, M. Minson, D. Hickey, K. Artyushkova, D. T. Glatzhofer and S. D. Minteer, *Acs Catal*, 2011, **1**, 1683-1690.
18. L. dos Santos, V. Climent, C. F. Blanford and F. A. Armstrong, *Phys Chem Chem Phys*, 2010, **12**, 13962-13974.
19. J. T. Holland, C. Lau, S. Brozik, P. Atanassov and S. Banta, *J Am Chem Soc*, 2011, **133**, 19262-19265.
20. T. Skalova, J. Dohnalek, L. H. Ostergaard, P. R. Ostergaard, P. Kolenko, J. Duskova, A. Stepankova and J. Hasek, *Journal of Molecular Biology*, 2009, **385**, 1165-1178.
21. J. Gallaway, I. Wheeldon, R. Rincon, P. Atanassov, S. Banta and S. C. Barton, *Biosens Bioelectron*, 2008, **23**, 1229-1235.
22. M. C. Machczynski, E. Vijgenboom, B. Samyn and G. W. Canters, *Protein Science*, 2004, **13**, 2388-2397.
23. D. Guan, M. Ramirez, L. Shao, D. Jacobsen, I. Barrera, J. Lutkenhaus and Z. Chen, *Biomacromolecules*, 2013, **14**, 2909-2916.
24. N. V. Sokolova and V. G. Nenajdenko, *Rsc Adv*, 2013, **3**, 16212-16242.
25. Y. Kim, S. H. Kim, D. Ferracane, J. A. Katzenellenbogen and C. M. Schroeder, *Bioconjug Chem*, 2012, **23**, 1891-1901.
26. S. Jung and H. Yi, *Biomacromolecules*, 2013.
27. X. Wu, B. Knudsen, S. M. Feller, J. Zheng, A. Sali, D. Cowburn, H. Hanafusa and J. Kuriyan, *Structure*, 1995, **3**, 215-226.
28. G. H. Zuo, W. Gu, H. P. Fang and R. H. Zhou, *J Phys Chem C*, 2011, **115**, 12322-12328.
29. N. Saifuddin, A. Z. Raziah and A. R. Junizah, *J Chem*, 2013, **2013**, 1-18.
30. J. Lin, I. A. Balabin and D. N. Beratan, *Science*, 2005, **310**, 1311-1313.
31. W. Wan, Y. Huang, Z. Y. Wang, W. K. Russell, P. J. Pai, D. H. Russell and W. R. Liu, *Angew Chem Int Edit*, 2010, **49**, 3211-3214.

